

Collaborative path planning and task allocation for multiple mowing robots in the standard orchards

Jinyan Xie¹, Shuteng Liu¹, Xiaosa Wang¹, Lixing Liu¹, Xu Wang¹, Jianping Li^{1,2}, Xin Yang^{1,2*}

(1. College of Mechanical and Electrical Engineering, Hebei Agricultural University, Baoding 071000, China;

2. Hebei Province Smart Agriculture Equipment Technology Innovation Center, Baoding 071001, China)

Abstract: Path planning and task allocation are the key technologies of multi-machine collaboration. Current approaches focus on field operations, but actually orchard operations are also a promising area. In order to improve the efficiency of orchard mowing, a cooperative operation scheduling method was proposed for multiple mowing robots in the dwarf dense planting orchards. It aims to optimize the non-working time of the robot in the intra-plot paths and inter-plot routes. Firstly, a genetic algorithm with multi-mutation and improved circle algorithm (MC-GA) was proposed for path planning. Subsequently, an ant colony optimization algorithm with mixed operator (Mix-ACO) was proposed for task allocation. With regard to the shortage of robots, a local search algorithm was designed to reassign work routes. Simulation experiment results show that MC-GA can significantly reduce the total turning time and the number of reverses for the robot. Mix-ACO can effectively allocate tasks by generating multiple work routes and reduce the total transfer time for the robot fleet. When the number of work routes exceeds the number of mowing robots, the local search algorithm can reasonably reallocate multiple routes to robots, reducing the difference in task completion time of the robot fleet. Field experiment results indicate that compared with the reciprocating method, SADG, and GA, MC-GA can reduce fuel consumption rate by 1.55%-8.69% and operation time by 84-776 s. Compared with ACO, Mix-ACO can reduce the total transfer time by 130 s. The research results provide a more reasonable scheduling method for the cooperative operation of multiple mowing robots.

Keywords: multiple mowing robot cooperation, complete coverage path planning, task allocation, combinatorial optimization problem, standard orchard

DOI: [10.25165/j.ijabe.20251802.9455](https://doi.org/10.25165/j.ijabe.20251802.9455)

Citation: Xie J Y, Liu S T, Wang X S, Liu L X, Wang X, Li J P, et al. Collaborative path planning and task allocation for multiple mowing robots in the standard orchards. Int J Agric & Biol Eng, 2025; 18(2): 218–230.

1 Introduction

Orchard grass is a soil management model which involves planting grass artificially in orchards to avoid soil exposure. It plays a positive role in improving soil conditions as well as increasing fruit yields. Thus, the economic benefits of planting grass are greater than those of clear tillage in orchards^[1]. To take advantage of grass planting, the techniques of orchard grass and mechanical mowing are often combined to achieve the cutting and returning of the grass to the field. However, the traditional mowing methods often require manual operation, which increases labor costs. It is time to introduce mowing robots in orchards to replace manual operations to alleviate the dependence of orchards on human labor and optimize management costs^[2-4]. With the growing maturity of

computer technology, sensor technology, and automatic control theory, more research^[5,6] has demonstrated the feasibility of orchard mowing robots. Meanwhile, fruit cultivation in China, such as apples, citrus, and cherries, is shifting towards the dwarf dense planting mode, making it easier for robots to operate. This is because in dwarf dense planting orchards, trees form a fixed operational structure, which allows robots to repeatedly perform operations to cover the entire orchard by moving along each row of trees from one end to another^[7].

The comprehensive operational efficiency of robots is the key to determining whether they are suitable for production^[8]. To improve the efficiency of orchard mowing, using multiple small mowing robots working together is more effective and energy-efficient^[9] than the method of increasing the mower's power and weight. In recent years, people have conducted more research on the collaborative operation of multiple agricultural machines of the same type, including intra-block multi-machine collaboration as well as inter-block multi-machine collaboration. Complete coverage path planning (CCPP) and task allocation, as the core issues for multi-machine collaboration, have become priorities in recent research. Effective path planning and task allocation can significantly improve the operational efficiency of agricultural machinery^[10].

The objective of CCPP is to achieve low operation costs and high operation efficiency when it seeks the optimal path to traverse the entire operation area^[11]. A field is completely covered by a set of parallel tracks or paths, which is the most commonly used field coverage mode for agricultural machinery^[12]. In this case, CCPP can be regarded as agricultural routing planning (ARP), which

Received date: 2024-10-24 Accepted date: 2025-02-14

Biographies: **Jinyan Xie**, MS candidate, research interest: agricultural mechanization engineering, Email: 20222090217@pgs.hebau.edu.cn; **Shuteng Liu**, MS candidate, research interest: agricultural mechanization engineering, Email: 20222090213@pgs.hebau.edu.cn; **Xiaosa Wang**, MS candidate, research interest: agricultural mechanization engineering, Email: 20222090216@pgs.hebau.edu.cn; **Lixing Liu**, PhD candidate, research interest: agricultural mechanization engineering, Email: 20211090024@pgs.hebau.edu.cn; **Xu Wang**, PhD candidate, research interest: agricultural mechanization engineering, Email: 20221090026@pgs.hebau.edu.cn; **Jianping Li**, Professor, research interest: automation of modern agricultural equipment, Email: ljpnd527@hebau.edu.cn.

***Corresponding author:** **Xin Yang**, PhD, Professor, research interest: modern agricultural equipment design and control, man-machine safety technology for ground machine systems. College of Mechanical and Electrical Engineering, Hebei Agricultural University, Baoding 071001, Hebei, China. Tel: +86-1593-345-9619, Email: yangxin@hebau.edu.cn.

determines the optimal path for agricultural machinery to travel in the field^[13]. It is difficult to obtain an exact solution for the ARP problem, so metaheuristic algorithms are often used to solve it^[14]. Different methods have been developed for ARP problems to realize various objectives in recent years. Bochtis et al.^[7] developed a route planning approach for orchard operations based on B-patterns to minimize the non-working distance traveled by an agricultural autonomous vehicle. Seyyedhasani et al.^[15] transformed the agricultural operation path planning problem into a vehicle routing problem and solved it by using a tabu search algorithm, reducing the field operation time by 17.3%. For specific agricultural activities, Conesa-Muñoz et al.^[16] used a simulated annealing algorithm to solve the path planning problem of site-specific herbicide spraying by an agricultural vehicle fleet. Evans et al.^[17] developed a genetic algorithm to optimize the harvest route of row crop harvesters and reduce operational costs. Zhang et al.^[6] proposed an improved A* algorithm to search optimal paths for multiple mowing robots in the same plot.

The essence of agricultural machinery task allocation is a resource scheduling problem with spatial and temporal characteristics, as well as resource constraints between agricultural machinery supply and farmland management demand^[18]. A large number of studies have shown that this problem can be transformed into a variant of the vehicle routing problem (VRP) based on the constraints to solve it. The VRP studies how to arrange vehicles to transport goods from warehouses to multiple geographically dispersed customer points or return goods to warehouses under certain constraints^[19]. Over the last few years, research on multi-agricultural machinery scheduling based on the VRP has expanded. Cao et al.^[20] used an ant colony algorithm to optimize the task sequence of agricultural machinery operation, which effectively reduced the path cost. Wang et al.^[21] proposed a multi-machine collaborative static task allocation method based on a multi-variation group genetic algorithm to reduce the work cost, including time, fuel consumption, and distance. He et al.^[22] applied a hybrid tabu search approach to optimize the scheduling plan for combine-harvesters of agricultural machinery cooperatives, which could reduce the wheat harvesting period by approximately 10%.

Research on path planning and task allocation for agricultural machinery is well-established. However, few studies seem to have considered the scheduling problem of multi-machine, multi-plot operations in orchard environments. The goal of this paper is to propose a multi-constraint scheduling method to solve the problem of collaborative operation for multiple mowing robots in dwarf dense planting orchards. The goal is achieved by focusing on intra-plot complete coverage path planning and inter-plot task allocation, and by considering several factors, namely, path costs, work capacity, matching supply and demand, and completion time.

2 Problem description

2.1 Overall research framework

In China, most orchards are located in hilly areas, with characteristics of highlighting topographic and geomorphic, small scale, and scattered plots. Therefore, during the mowing season, it is more convenient and flexible to use compact and lightweight mowing robots for operation instead of large mowing machines. It can greatly improve the mowing efficiency to use multiple mowing robots to work together in fragmented and dispersed plots. However, during actual orchard operations, the path planning and task allocation for the robot fleet is an optimization problem influenced by multiple factors. This paper considers the following

factors in relation to the actual situations:

1) Path cost: The row spacing of fruit trees is about 3.5-4.0 m, and the working width of the mowing robot is relatively small. So, each inter-row corridor needs to be operated twice back and forth. In order to maintain moisture, increase temperature, and suppress weed growth, a black ground cloth approximately 2 meters wide is also placed along the row of fruit trees. It will result in uneven track spacing (here, the term "row" refers to a group of trees parallel to the direction of robot operation, and "track" refers to the operation path starting from one end and ending at the other end, with tracks existing in the row space). Therefore, there are different turning costs for the mowing robot between intra-row and inter-row. Similarly, the plots in the orchard are scattered, so the transfer costs for the mowing robot to operate across the plots are different.

2) Work capacity: The small size of orchard mowing robots requires that they operate within fuel capacity limits without exceeding their capacity.

3) Supply and demand matching: If the number of mowing robots in the orchard garage is not enough to complete all tasks in one trip, it is necessary to consider the scenario where the fleet members complete all tasks in multiple trips.

4) Completion time: It is important to consider whether the workload for each member is balanced when assigning tasks to the robot fleet. The purpose is to avoid unfair treatment of one mowing robot that may experience extremely long or short working hours.

To address these constraints, the framework of this paper is illustrated in Figure 1. Firstly, based on the ARP model^[13], a genetic algorithm with multi-mutation and improved circle algorithm (MC-GA) is proposed to plan the intra-plot complete coverage path. The algorithm aims to minimize the non-working time of the mowing robot while working in the plot. Subsequently, based on the capacitated vehicle routing problem (CVRP) model, an ant colony optimization algorithm with mixed operator (Mix-ACO) is proposed for task allocation. The algorithm aims to minimize the non-working time of the mowing robot while transferring between plots. Finally, considering the situation where all tasks cannot be completed in one trip due to the shortage of mowing robots, each robot needs to operate continuously multiple times to complete the tasks on multiple routes. A local search algorithm is designed to perform the second task allocation by reassigning work routes. The algorithm aims to minimize the difference in task completion time among the members of the robot fleet, and find the complete work routes for each mowing robot to complete all tasks in multiple trips.

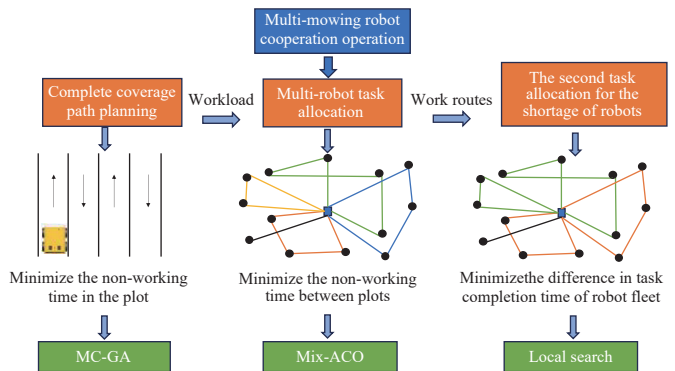
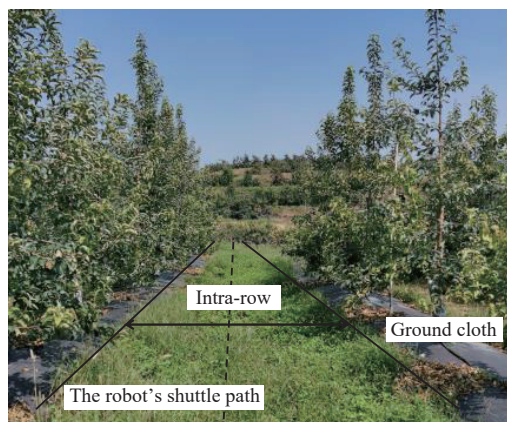


Figure 1 Overall framework of the research program

2.2 Complete coverage path planning

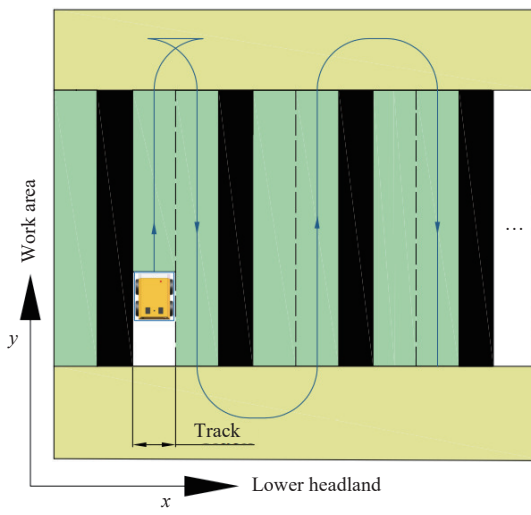
The results of path planning determine how a mowing robot covers a plot. A reasonable path can effectively reduce non-working time. As shown in Figure 2, a plot can be divided into two parts,

including working area and non-working area. The working area is the area that needs to be mowed, while the non-working area includes the ground cloth coverage area and two field edges. The headland serves as the turning area for the mowing robot. The upper headland is labeled UH, and the lower one is labeled LH. The mowing robot operates twice in each row. If there are n rows of fruit trees, it must traverse $2n$ tracks to completely cover them. It is assumed that (x_1^k, y_1^k) represents the horizontal and vertical coordinates of the first fruit tree in the k -th row, and (x_2^k, y_2^k) represents the horizontal and vertical coordinates of the last fruit tree in the k -th row, where $1 \leq k \leq n$. The coordinates of the fruit trees at both ends of each row can be represented by a two-dimensional matrix. Therefore, based on the Global Navigation Satellite System, the boundary between the headland and the working area can be determined.



a. A dwarf dense planting orchard

Upper headland

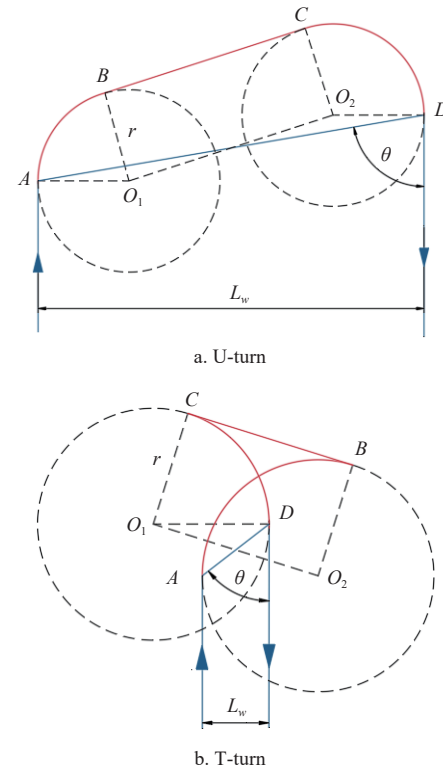


b. Schematic of a mowing robot working scene

Figure 2 Scenario analysis

When an orchard mowing robot drives to the end of the track, it needs to make a 180° turn at the headland before entering the next track. According to reference [12], a large portion of the non-working time for agricultural machinery occurs during turning, while the non-working time during turning mainly depends on the driving distance and average speed during turning. As this indicates, the choice of turning patterns is important. Due to the easy operation of some turning types, they can be quickly executed by machine, while others require good driving skills and a large area of field edge to perform. The most common turning patterns are the forward-turn (Ω -turn), double round corner (U-turn), and switch-

back-turn (T-turn)^[12]. Usually, the latter two types of turns will be initiated only when the U-turn cannot be executed. For example, when $L_w < 2r$, where L_w is the spacing between the current track and the next track, and r is the minimum turning radius of the machine, the width of the headland and the length of the path occupied by the Ω -turn are much larger than those of the T-turn^[14]. Based on a comprehensive comparison, only the U-turn and T-turn are considered for use in this paper, with their turning principles shown in Figure 3.



Note: O_1 and O_2 represent the centers of the auxiliary circles; A , B , C , and D represent the tangent points of the turning path to circles O_1 and O_2 .

Figure 3 Schematic of turning patterns

As shown in Figure 3, when the mowing robot travels to the end of the track, its driving direction will form an angle θ with the boundary of the headland. If the angle θ is less than 90° , the robot will use the U-turn or T-turn with an inclination angle θ in the process of entering the next track. If the angle θ is equal to 90° , the normal U-turn or T-turn will be used. The former turning method is suitable for irregular plots, while the latter is more suitable for rectangular plots^[23]. The tracks within the plot are parallel to each other. Generally speaking, as long as the boundary of the headland is determined, the angle θ can be obtained through measurement in advance. The traditional approach commonly adopts the reciprocating scheduling strategy for each row, which often needs to be used with the T-turn. However, the T-turn involves stopping and reversing, which not only consumes more time but also increases the wear on the tires due to soil friction. Therefore, it is advisable to avoid the T-turn as much as possible during actual operations. This objective can be achieved by optimizing the mowing robot's traversal order across the tracks.

2.3 Multi-robot task allocation

Task allocation requires establishing a clear mapping relationship between multiple agricultural machines and multiple plots to be operated^[20]. Therefore, firstly, the workload of each plot needs to be obtained based on the path planning result. Then, the

path cost is calculated based on the distance between the mowing robot and each plot. Finally, considering the workload, path cost, work capacity, and supply and demand matching, a global scheduling model is established with short paths, high efficiency, and reasonable configuration.

A batch of mowing robots is parked and scheduled uniformly in the orchard, allowing multiple robots to complete multiple tasks in parallel. According to [24], it can be described as the ST-SR-TA problem (single-task robots, single-robot tasks, time-extended assignment). Each plot in the orchard is considered as a task unit, and the information for each task is known. Each task can only be operated by one mowing robot, while one mowing robot can be assigned multiple tasks. The objective is to allocate the tasks to each robot so as to minimize the transfer time taken by a robot to serially execute its allocated tasks. Furthermore, considering practical application scenarios, some constraints have been added. The fuel capacity of each robot determines the number of tasks it can perform in one trip. When assigning tasks to the robot fleet, it is necessary to consider the workload of each plot and the current remaining capacity of the robot. Once the robot's capacity reaches the lower limit, it must return to the garage. Of course, it can also return to the garage after all tasks are completed. As shown in Figure 4, the fleet of mowing robots departs from the garage at the same time and serves multiple plots in the orchard in an organized manner, following a preset work route. Due to fuel capacity constraints, each mowing robot can only service a limited number of plots at a time, and when they run out of fuel, they need to return to the garage for refueling before starting a new trip. Therefore, plots on the same-colored route in Figure 4 indicate that they are serviced by the same mower. When there are not enough mowers in the orchard, one mower is often responsible for plots on multiple routes.

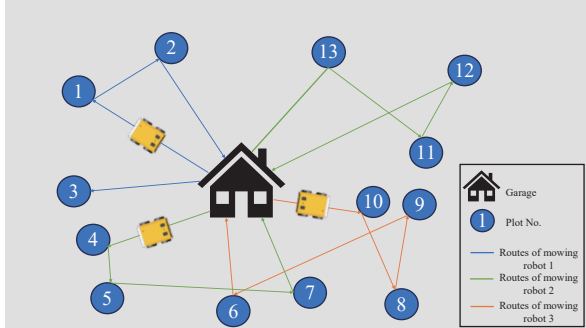


Figure 4 Schematic of the collaborative operation scenario for multiple mowing robots

In summary, in order to simplify the problem to facilitate model calculation, the following assumptions are proposed:

- 1) In task allocation, each plot can only be mowed by one robot, but one robot can serve multiple plots.
- 2) An orchard has only one garage, and all the mowing robots depart from the garage at the same time, returning to it after completing their assigned tasks.
- 3) There are no obstacles in the plots and roads of the orchard. During the operation, the parameters of the robot fleet are the same and not affected by external factors, without experiencing malfunctions.
- 4) All roads are wide enough to be used by multiple mowing robots simultaneously to avoid collisions during the transfer process.

5) The plots are not interconnected. The mowing robot can only enter and exit the plots through the designated entrance/exit.

6) The plot can only be allocated when the remaining fuel of the mowing robot is sufficient to complete the task. If there is no suitable plot, the mowing robot needs to return to the garage to replenish fuel.

3 Methods and materials

3.1 Complete coverage path planning within the plot

3.1.1 Mathematical model

The parallel tracks in the plot are regarded as the nodes to be traversed by the mowing robot. When the robot visits the node, it also completes the operation of the track at the same time. Let N be the set of nodes and E be the set of edges connecting the nodes. The cost matrix C is associated with each edge, where c_{ij} represents the time cost of the mowing robot to travel from node i to node j , $\forall i, j \in N$. x_{ij} is a decision variable, with $x_{ij}=1$ if and only if the mowing robot transfers from node i to node j , and $x_{ij}=0$ otherwise. The solution to the ARP problem is to determine the shortest path for the mowing robot to traverse all tracks. $R = \{R_1, R_2, \dots, R_{|N|}\}$ is assumed as a path for the mowing robot, where R_i is the node to be traversed. The path optimization model can be described as follows:

$$\text{Minimize} \sum_{i \in N} \sum_{j \in N} c_{ij} x_{ij} \quad (1)$$

Subject to:

$$\sum_{j \in N} x_{ij} = 1; \forall i \in R \quad (2)$$

$$R_0 = R_{|N|+1} = 1, \text{ and } \{R_1, R_2, \dots, R_{|N|}\} \subseteq N \quad (3)$$

$$\sum_{i \in N} \sum_{j \in N} x_{ij} \leq |S| - 1; \forall S \subseteq N, |S| > 1 \quad (4)$$

$$x_{ij} \in \{0, 1\}; \forall i, j \in N \quad (5)$$

The time for a mowing robot to cover a plot consists of two parts, namely, the working time on the tracks and the turning time between the tracks. When the environment is determined, the working time is constant, so the main focus needs to be on the turning time. The objective function [Equation (1)] aims to minimize the total turning time when the robot covers the plot. Equation (2) ensures that each track represented by a node is traversed only once. The first track near the entrance/exit of the plot is regarded as node 1. To simplify operations and avoid adding new nodes, Equation (3) specifies that the mowing robot starts at node 1 and returns to node 1 after completing the task. Equation (4) excludes disjoint sub-loops from a feasible solution. Finally, Equation (5) specifies that the decision variables only use binary values.

The time cost matrix C is composed of the working time and the turning time. When $i=j$, c_{ij} represents the working time required for the mowing robot on the track. When $i \neq j$, c_{ij} represents the turning time required for the mowing robot to transfer from node i to node j . At this point, there are two possibilities: 1) the mowing robot turns at the headland UH; 2) the mowing robot turns at the headland LH. In the rectangular plots, fruit trees are symmetrically distributed on both sides of the headland, so $c_{ij}^{UH} = c_{ij}^{LH}$. In the irregular plots, fruit trees are asymmetrically distributed on both sides of the headland, so $c_{ij}^{UH} \neq c_{ij}^{LH}$. Thus, the time cost matrix C is expressed as follows:

$$C = \begin{bmatrix} c_{11} & \infty & c_{12}^{\text{UH}} & \infty & \cdots & c_{1|N|}^{\text{UH}} & \infty \\ \infty & c_{11} & \infty & c_{12}^{\text{LH}} & \cdots & \infty & c_{1|N|}^{\text{LH}} \\ c_{21}^{\text{UH}} & \infty & c_{22} & \infty & \cdots & c_{2|N|}^{\text{UH}} & \infty \\ \infty & c_{21}^{\text{LH}} & \infty & c_{22} & \cdots & \infty & c_{2|N|}^{\text{LH}} \\ \vdots & \vdots & \ddots & \vdots & \ddots & \vdots & \vdots \\ c_{|N|1}^{\text{UH}} & \infty & c_{|N|2}^{\text{UH}} & \infty & \cdots & c_{|N||N|}^{\text{UH}} & \infty \\ \infty & c_{|N|1}^{\text{LH}} & \infty & c_{|N|2}^{\text{LH}} & \cdots & \infty & c_{|N||N|}^{\text{LH}} \end{bmatrix} \quad (6)$$

The calculation of c_{ij}^{UH} or c_{ij}^{LH} is related to the turning strategy employed. When $L_w \geq 2r$, the U-turn is used; otherwise, the T-turn is used. In this context, Equation (7) or (8) is used to calculate the turning time required for the robot at the headland. It is worth noting that the angle θ is set based on the specific characteristics of the plot.

$$U_{ij} = \frac{\pi r + \sqrt{(d_{i,j}w + zL_d - 2r)^2 + (d_{i,j}w + zL_d)^2 \cot^2 \theta}}{v_t} \quad (7)$$

$$T_{ij} = \frac{\pi r + \sqrt{(2r - d_{i,j}w - zL_d)^2 + (d_{i,j}w + zL_d)^2 \cot^2 \theta}}{v_a} \quad (8)$$

where, U_{ij} is the U-turn time, (s); T_{ij} is the T-turn time, (s); $d_{i,j}$ is the span between the two tracks during turning, $d_{i,j} = |i-j|$, $i \neq j$; w is the working width of the mowing robot, (m); z is the number of ground cloths crossed by the mowing robot during turning; L_d is the width of the ground cloth, (m); v_t is the turning speed of the mowing robot without reversing, (m/s); v_a is the average turning speed of the mowing robot when it is in reverse, (m/s); θ is the angle between the driving direction of the robot and the boundary of headland, (°).

Next follow the calculation formulas for the time cost t_{start} (from node 1 to the first track) and the time cost t_{back} (back to node 1 from the end of the last track).

$$t_{\text{start}} = c_{1R_1}^{\text{UH}} \quad (9)$$

$$t_{\text{back}} = \begin{cases} c_{1R_{|N|}}^{\text{UH}}, & \text{turning at the UH} \\ c_{R_{|N|}1}^{\text{LH}} + c_{11}, & \text{turning at the LH} \end{cases} \quad (10)$$

3.1.2 Algorithm description

The genetic algorithm is the most popular algorithm for solving the agricultural routing planning (ARP) problem^[23], and is adopted in this paper. The genetic algorithm is the search algorithm based on population optimization that imitates the genetic evolution process of natural organisms^[25]. Inspired by biology, chromosomes are represented as the solutions to the problem in the genetic algorithm, which are evaluated with the fitness value. Then, the genetic algorithm regards the population as the solution set, updating it through the process of selection, crossover, and mutation in order to ultimately select the individual with the best fitness in the population.

The track sequence in route R is encoded using natural number codes as the genes of the chromosome. Therefore, a chromosome can be represented by the set $R = \{R_1, R_2, \dots, R_{|N|}\}$ as shown in Figure 5. After the formation of the population, the fitness function is defined as the total turning time when the mowing robot covers the plot. The chromosomes with smaller fitness values indicate better path optimization effects, and the chromosome with the lowest fitness value represents the best path solution.

The selection operator determines whether the chromosomes are involved in the next generation reproduction or not. Usually, the genetic algorithm selects the parent based on the fitness value of each chromosome. Tournament selection is used to select the parent

chromosomes in this paper. Compared with other selection strategies, tournament selection is more suitable for solving minimization problems and simple to implement. After using the tournament selection strategy to select a group of chromosomes as the group of parents, a mutation operator is still required to generate offspring. Traditional genetic algorithms select different mutation operators by mutation probability. In this paper, a variety of mutation operators (Swap, Insertion, Inversion) are used to generate multiple offspring instead of choosing one operator, which increases the population diversity while updating the population. Figure 6 describes the process of mutation.

Track sequence										
Chromosome	2	5	8	10	7	4	1	3	6	9

Figure 5 Schematic of track coding

Parent chromosome	2	5	8	10	7	4	1	3	6	9
Swap: swap the path code positions at a and b	a	Randomly selecte locations a and b						b		
Insertion: insert the path code a after b										
Invesion: invert the path code between a and b										
Offspring 1	2	3	8	10	7	4	1	5	6	9
Offspring 2	2	8	10	7	4	1	3	5	6	9
Offspring 3	2	3	1	4	7	10	8	5	6	9

Figure 6 The process of chromosome mutation

To enhance the algorithm's ability to quickly find the optimal solution, the improved circle algorithm is employed to optimize the parent chromosomes. The improved circle algorithm is a heuristic algorithm. Its principle involves modifying the path node order in a Hamiltonian cycle once, resulting in a Hamiltonian cycle with a shorter path length. By repeatedly modifying it, an approximately optimal operating path is obtained. Therefore, if the parent chromosome is optimized by the improved circle algorithm, its fitness value must be inevitably better than that before optimization.

Table 1 lists the pseudocode of the genetic algorithm based on multi-mutation and improved circle algorithm (MC-GA). The details are indicated as follows:

- 1) Input the information of the plots and the mowing robot to generate time cost matrix.
- 2) Set the algorithm parameters and initialize the population.
- 3) Determine whether the maximum number of iterations has been exceeded. If so, proceed to step (9); otherwise, perform steps (4)-(8).
- 4) Calculate the fitness value of each individual in the current population and retain the best individual of the population.
- 5) Based on the tournament selection method, randomly select four chromosomes to form a group for comparison, retain the individual with the lowest fitness value as the parent, and then use the improved circle algorithm to optimize the parent chromosome.
- 6) Use multiple mutation operators to mutate the optimized parent chromosome multiple times to generate multiple offspring.
- 7) Repeat steps (5)-(6) until a new population is formed.
- 8) Increment the iteration count and skip to step (3).
- 9) Output the path of the best individual.

Table 1 The pseudocode of MC-GA**Algorithm 1** MC-GA

```

1: Input the information of the plots and the mowing robot
2: Set the parameters
3: pop=zeros (popSize, :)
4: globest=Inf
5: offspring=zeros (4, :)
6: newpop=zeros (popSize, :)
7: pop=randperm (popSize, :)
8: while iter<=iter_max do
9:   Calculate the path cost of each individual in pop
10:  curbest←Min(cost)
11:  curbest_path ← Min(cost)_path
12:  if curbest< globest then
13:    globest← curbest
14:    globest_path← curbest_path
15:  end if
16:  randomorder=randperm(popSize)
17:  for i= 4:4: popSize do
18:    bestparent←Tournament_Selection (pop (randomorder (i-3: i)))
19:    optparent←Improved Circle Algorithms(bestparent)
20:    offspring (1, :)← optparent
21:    offspring (2, :)←Swap (optparent)
22:    offspring (3, :)←Insertion (optparent)
23:    offspring (4, :)←Inversion (optparent)
24:    newpop (i-3: i, :)=offspring
25:  end for
26:  pop=newpop
27:  iter=iter+1
28: end while
29: Output the globest and globest_path

```

3.2 Multi-robot task allocation among the plots

3.2.1 Mathematical model

In the orchard, multiple mowing robots with limited fuel capacity depart from the garage simultaneously to service multiple scattered plots in turn. If the plots are regarded as customers and the fuel as goods, this scheduling problem can be transformed into the famous capacitated vehicle routing problem (CVRP), which is also a combinatorial optimization problem in essence. Therefore, the assumptions made in the previous section are continued, but expanded to include the entire orchard, not just a specific plot.

In mathematical terms, CVRP is represented as a weighted graph $G=\{N, E\}$, where $N=\{0, 1, 2, \dots, n\}$ is the set of nodes, and $E=\{(i, j)|i, j \in N\}$ is the set of arcs. In this context, the garage is represented as the node 0, and the n plots to be served are represented by other nodes. The cost matrix C is associated with each edge; when $i \neq j$, c_{ij} represents the time cost for the mowing robot to travel from node i to node j , and when $i=j$, c_{ii} represents the time for the mowing robot to cover each plot. The demand at the garage is set to zero. Ideally, the single working time of the mowing robot is only determined by its fuel tank capacity. So, a common endurance time limit L for each robot was given. The power system of the mowing robot can be divided into the working power system (driven by an engine) and the traveling power system (driven by a battery pack). Therefore, the fuel consumption during the transfer process is not considered, while the endurance time does not include transfer time. The objective of the CVRP is to determine a set of lowest-cost routes to service all plots while satisfying constraints. Assuming that K routes have been determined, and $T = \{T^1, T^2, \dots, T^K\}$ is the set of these routes, then the k -th route can be represented as $T^k = \{T_1^k, T_2^k, \dots, T_{|T^k|}^k\}$, where T_i represents the node to be visited. Variable y_{ij}^k is equal to 1 if the mowing robot moves from node i to node j in route k , and 0 otherwise. Variable l_{ij}^k is equal to 1 if the mowing robot services node i in route k , and 0 otherwise.

The task allocation model can be described as follows:

$$\text{Minimize} \sum_{i=0}^n \sum_{j=0}^n \sum_{k=1}^K c_{ij} y_{ij}^k \quad (11)$$

Subject to:

$$\sum_{k=1}^K \sum_{j=1}^n y_{ij}^k = 1; \quad \forall i \in \{1, \dots, n\} \quad (12)$$

$$\sum_{k=1}^K \sum_{i=1}^n y_{ij}^k = 1; \quad \forall j \in \{1, \dots, n\} \quad (13)$$

$$\sum_{j=1}^n y_{0j}^k = 1; \quad \forall k \in \{1, \dots, K\} \quad (14)$$

$$\sum_{i=1}^n y_{i0}^k = 1; \quad \forall k \in \{1, \dots, K\} \quad (15)$$

$$\sum_{i=0}^n \sum_{j=0}^n c_{ij} l_{ij}^k \leq L; \quad \forall k \in \{1, \dots, K\} \quad (16)$$

The objective function [Equation (11)] aims to minimize the total transfer time of the robot fleet when they operate across plots. Equations (12) and (13) ensure that each plot represented by a node is visited exactly once. Equations (14) and (15) require all routes to begin and end at the garage. Equation (16) ensures that the total demand on each route does not exceed the endurance time limit L of the robot.

Although the use of CVRP can help solve the multi-robot task allocation problem, the solution provided by CVRP only involves a group of robots completing all tasks in one trip, without considering the situation where there is a shortage of robots. It implies that even if K routes have been planned based on capacity constraints, the actual number of robots M may be less than K , so not all tasks can be completed in one trip. Therefore, a second allocation for the set T of work routes is required based on the actual number of mowing robots. Firstly, the work routes need to be packed, and the time consumption on the k -th route is expressed as $H(k)$ [Equation (17)]. Then, the K routes are assigned to M mowing robots. To avoid uneven allocation, each mowing robot is assigned to P routes at least [Equation (18)]. The completion time of the m -th mowing robot to complete all tasks is indicated as $t(m)$ [Equation (19)]. Finally, with the objective of minimizing the difference in task completion time of the robot fleet, the complete work routes are determined for each mowing robot to complete all tasks in multiple trips. The difference in task completion time of the robot fleet is calculated by Equation (20), where the average completion time for all mowing robots is given by $\left(\sum_{i=0}^n \sum_{j=0}^n \sum_{k=1}^K c_{ij} y_{ij}^k + \sum_{i=1}^n c_{ii} \right) / M$. The objective function [Equation (21)] is used to minimize the difference in task completion time of the robot fleet. Constraint Equation (22) guarantees that there is only one mowing robot on each route.

$$H(k) = \sum_{i=0}^{|T^k|} \sum_{j=0}^{|T^k|} c_{ij} y_{ij}^k + \sum_{i=1}^{|T^k|} c_{ii}; \quad \forall k \in \{1, \dots, K\} \quad (17)$$

$$P = \left\lfloor \frac{K}{M} \right\rfloor \quad (18)$$

$$t(m) = \sum_{i=1}^p H(k); \quad \forall m \in \{1, \dots, M\} \quad (19)$$

$$\alpha(m) = \frac{\left(\sum_{i=0}^n \sum_{j=0}^n \sum_{k=1}^K c_{ij} y_{ij}^k + \sum_{i=1}^n c_{ii} \right) / M - t(m)}{\left(\sum_{i=0}^n \sum_{j=0}^n \sum_{k=1}^K c_{ij} y_{ij}^k + \sum_{i=1}^n c_{ii} \right) / M} \quad (20)$$

$$\text{Minimize}(\max(\alpha) - \min(\alpha)) \quad (21)$$

$$\bigcap_{m=1}^M T^k = \{0\} \wedge \bigcup_{m=1}^M T^k = T; \quad \forall k \in \{1, \dots, K\} \quad (22)$$

3.2.2 Algorithm description

1) Ant colony optimization algorithm with mixed operator

During the foraging process, ants will secrete pheromones along their paths. The magnitude of the pheromone concentration reflects the distance of the path, and the higher the pheromone concentration, the shorter the corresponding path distance. As a result, the ant colony algorithm possesses the characteristics of distributed computing, positive information feedback, and heuristic search, making it a probabilistic algorithm that can be used to find optimal solutions^[26]. When using the ant colony algorithm, artificial ants make probabilistic decisions based on the problem information, pheromone trails, and heuristic information. Specifically, for CVRP, each artificial ant builds its complete route by successively selecting feasible nodes through probability calculation and roulette wheel strategy until all nodes have been visited. When all the artificial ants construct a complete route, each route needs to be converted into a corresponding allocation scheme by decoding it. In the process, capacity constraints are always adhered to. If the current remaining capacity fails to meet the demand of the next node, a new work route will be initiated from the garage. Thus, each artificial ant represents a solution, while each solution includes several work routes due to the capacity constraints. Then by costing each solution, the one with the lowest cost can be selected as the best solution.

In fact, for the combinatorial optimization problems, the ant colony algorithm has the best performance when combined with local search operators^[27]. Therefore, several classical permutation operators have been combined to propose a mixed operator, including Swap, Insertion, Inversion, and Displacement. The mixed operator improves the best solution by assisting the ant colony algorithm in searching the neighborhood. **Table 2** gives a brief introduction to these operators. The mixed operator combines the four operators into one, and simultaneously classifies them into two categories, including single relocation (Swap, Insertion) and segment relocation (Inversion, Displacement). Single relocation makes slight changes to improve the solution, which is usually effective in the last stages of the search, while segment relocation makes large changes to widely explore the solution space, which is effective in the early stages of the search^[28]. In summary, the mixed operator is expressed by Equation (23). Obviously, in the process of

each algorithm iteration, the mixed operator will choose which operator to use by roulette wheel strategy to explore the neighborhood, instead of always using the same operator. In order to make better use of the characteristics of the mixed operator, the probability of segment relocation being selected is increased in the early stage of the algorithm iterations. However, it is different from this in the later stage, which facilitates the ant colony algorithm to better escape the current local optimal solution.

$$\text{mix-opt}(x) = \begin{cases} \text{single swap}(x), & \text{if } r \leq \sum_{i=1}^1 p(x_i) \\ \text{single insertion}(x), & \text{else if } r \leq \sum_{i=1}^2 p(x_i) \\ \text{segment inversion}(x), & \text{else if } r \leq \sum_{i=1}^3 p(x_i) \\ \text{segment displacement}(x), & \text{else if } r \leq \sum_{i=1}^4 p(x_i) \end{cases} \quad (23)$$

where, $r \in [0,1]$ is a randomly generated number, and $p(x_i)$ is the probability of each operator being selected.

Table 2 Most common permutation operators

Name	Description
Swap	Interchanges two elements
Insertion	Relocates one element to a random position
Inversion	Reverses several consecutive elements
Displacement	Relocates several consecutive elements to a random position

The pheromone trails will be updated after the best solution has been optimized by the mixed operator, providing a reference when planning the routes again. The purpose of pheromone update is to make well-performing routes more popular in the following iterations, and includes pheromone evaporation and pheromone deposition. At present, the research on ant colony algorithm mainly uses ant-cycle. That is, pheromone update is carried out only after all ants have constructed their complete routes, and the number of pheromones deposited by each ant is set as a function of the route quality^[27]. The better the route, the higher the pheromone concentration. In order to improve the efficiency of the algorithm, the elite ant strategy is used to update the pheromones. Only the best-performing ants can evaporate and deposit the pheromones on the edge (i, j) they pass through, so as to avoid the sub-optimal route being overemphasized. Thus, pheromone update function can be expressed by Equation (24).

$$\tau_{i,j}(\text{iter} + 1) = (1 - \rho)\tau_{i,j}(\text{iter}) + Q/T_{\text{bestR}}; \quad i, j \in \text{bestR} \quad (24)$$

where, $\tau_{i,j}$ is the pheromone concentration on the edge (i, j) ; iter is the current number of iterations; $\rho \in [0,1]$ is the pheromone evaporation factor; Q is a constant; and T_{bestR} is the transfer time of the best route.

The pseudocode of the ant colony optimization algorithm with mixed operator (Mix-ACO) is listed in **Table 3**. The specific steps are as follows:

- (1) Create the cost matrix, i.e., estimate transfer time using Manhattan distance and coverage time using MC-GA.
- (2) Set the parameters of Mix-ACO, and initialize the pheromone matrix and route record table.
- (3) Determine whether the maximum number of iterations has been exceeded. If so, proceed to step (4); otherwise, perform the

following actions:

- (a). Construct and record the route of each ant, and calculate the total transfer time of each scheme by decoding the route of each ant;
- (b). Select the task allocation scheme with the lowest cost as the best one and optimize it using the mixed operator;
- (c). Update the pheromone matrix by updating the pheromones on the best route;
- (d). Record the best task allocation scheme;
- (e). Reset the route record table and increment the iteration count.
- (4) Output the optimal task allocation scheme.

Table 3 The pseudocode of Mix-ACO

Algorithm 2 Mix-ACO

```

1: Input the information of the nodes and the mowing robot
2: Initialize the algorithm parameters
3: globest=Inf
4: while iter<=iter_max do
5:   for i=1: antSize do
6:     Construct and record the route for each ant
7:   end for
8:   for i=1: antSize do
9:     corresponding allocation scheme←Decode(route)
10:    cost←CostFun(scheme)
11:   end for
12:   curbest←Min(cost)
13:   curbest_route ← Min(cost)_route
14:   if curbest<globest then
15:     globest← curbest
16:     globest_route← curbest_route
17:   end if
18:   globest_route←Mix-opt(globest_route)
19:   Tau←UpdateTau (globest_route)
20:   iter=iter+1
21: end while
22: best _scheme←Decode(globest_route)
23: Output the best_scheme

```

2) Local search

Local search (LS) is a heuristic algorithm for solving optimization problems, which is simple, flexible, and easy to implement. Therefore, this algorithm is used to reassign the work routes. Local search starts with a complete initial solution and attempts to find a better solution in an appropriate neighborhood of the current solution^[29]. Based on the first task allocation results, K work routes are randomly assigned to M mowing robots by using a separator operator, so as to generate the initial solution of the algorithm. Then the initial solution is assigned to the global optimal solution. Next, a swap operator is used to generate a new solution. If the new solution is better than the current solution, the current solution will be replaced with the new solution, updating the global optimal solution. Then, the operation is repeated until the algorithm terminates. Finally, the global optimal solution is output.

3.3 Case study

In this section, a case study is presented to verify the feasibility of the proposed methods. The tests include both simulation experiments and field experiments.

3.3.1 Study location and equipment

The experiments were conducted in the Modern Science and Technology Agricultural Park (38°58'17.0436"N, 114°54'31.6116"E),

which is located in Shunping County, Baoding City, Hebei Province, China. The information of the experimental site was provided by ArcGIS Earth software. Sixteen relatively flat regular or irregular plots were selected in the orchard as the experimental objects. The plots were numbered (Figure 7), with the red area indicating the coverage area of the plots, the blue solid line representing the plot boundaries, and circular markers indicating the entrances/exits of the plots. The position of each node was in the WGS-84 coordinate system (Table 4), and the distance between nodes was calculated by longitude, latitude, and elevation coordinates. Due to terrain constraints, the distance between two nodes cannot be represented by linear distance. Therefore, Manhattan distance was used to calculate the distance between nodes, which needs to be converted from the WGS-84 coordinate system to the Cartesian coordinate system before calculation.



Figure 7 Schematic map of study area

Table 4 Longitude, latitude, and elevation coordinates of all nodes in the orchard

Node number	Coordinate (X-axis/long.-E, Y-axis/lat.-N, Z-axis/ele.)
0	(114.908 415, 38.971 661, 278.98)
1	(114.908 948, 38.972 666, 281.16)
2	(114.909 036, 38.972 249, 278.85)
3	(114.909 019, 38.971 582, 273.59)
4	(114.909 232, 38.971 253, 270.85)
5	(114.909 044, 38.971 211, 272.68)
6	(114.909 659, 38.970 736, 264.93)
7	(114.909 555, 38.971 052, 266.02)
8	(114.909 776, 38.971 225, 267.45)
9	(114.910 019, 38.970 942, 261.98)
10	(114.910 381, 38.970 563, 259.96)
11	(114.911 615, 38.970 093, 253.63)
12	(114.911 732, 38.970 113, 253.42)
13	(114.912 468, 38.970 053, 250.35)
14	(114.912 329, 38.970 546, 255.64)
15	(114.912 686, 38.970 625, 251.56)
16	(114.912 350, 38.970 814, 256.51)

The simulation experiments were conducted on a computer with the Windows 11 operating system, an AMD Ryzen 7-5800H at 3.20 GHz, 16 GB of RAM, and an NVIDIA GeForce GTX 3050 GPU. MATLAB (R2023a, MathWorks, USA) was used to conduct the algorithm simulations.

The equipment used in the field experiments was the G33 remote-controlled mower manufactured by Qiangshi (Shanghai, China) Technology Co., Ltd. So in the field experiments, scheduling

of the mower was achieved by manual remote control. The parameters of the mower were obtained by taking the average value of several measurements in the field: the endurance time is $L=3.5$ h, the working width is $w=1.0$ m, the minimum turning radius is $r=2.0$ m, the driving speed on the road is $v=1.1$ m/s, the operational speed is $v_w=0.7$ m/s, the turning speed without reverse is $v_t=0.4$ m/s, and the average turning speed with reverse is $v_a=0.24$ m/s. The working scene of the G33 mower is shown in Figure 8.



Figure 8 Actual working scene of G33 mower in the orchard

3.3.2 MC-GA simulation experiments

The reciprocating method is a conventional path planning method, where the robot executes adjacent track sequence to cover the entire area^[10]. However, this method is not optimal in an orchard with limited operational space. Firstly, the MC-GA was compared with the reciprocating method to verify its effectiveness. The path planning experiments were conducted on the randomly selected plots No.1, No.5, No.10, No.14, and No.16. The parameters of MC-GA were set as follows: the population size is 40 while the number of iterations is 500. The parameters of the mowing robot were set as follows: the working width is $w=1.0$ m, the minimum turning radius is $r=0.8$ m, 0.9 m, and 1.0 m, the operational speed is $v_w=1.35$ m/s, the turning speed without reverse is $v_t=1.1$ m/s, and the average turning speed with reverse is $v_a=0.6$ m/s.

Secondly, in order to verify the superiority of MC-GA, the algorithms SADG, IPSO (as proposed in the literature [30, 31]), and basic GA were used for comparison with MC-GA proposed in this paper. Similarly, plots No.1, No.5, No.10, No.14, and No.16 were selected. The algorithm parameters were set as follows: for SADG, the initial temperature is 100°C, and the cooling factor is 0.95; for IPSO, the maximum value of inertia weight is 1; for GA, the selection probability is 0.5, the crossover probability is 0.9, and the mutation probability is 0.1. The size of each algorithm is 40 with 500 iterations. The average result of 10 runs of each algorithm was taken as the final result.

3.3.3 Mix-ACO simulation experiments

In order to evaluate the workload of each plot, the MC-GA was utilized to calculate the total turning time for each node. Subsequently, the time for the mowing robot to cover each node was further estimated based on the area of the plot, as shown in Table 5.

In theory, task allocation can be achieved based on the corresponding node sequence after inputting the acquired node information into the Mix-ACO. There are two cases which were considered for simulation experiment validation:

1) Scenario 1: Number of work routes less than number of mowing robots

The number of tasks were randomly set to 4, 7, 10, 13, and 16, respectively. The working parameters of the mowing robot were set as follows: the endurance time is 1.2/1.5 h, and the driving speed on the road is $v=1.35$ m/s. The parameters of Mix-ACO were set as follows: the importance factor of pheromones is 1, the importance factor of the heuristic function is 3, the evaporation factor of pheromones is 0.15, the constant to update the pheromone concentration is 5, the number of ants is 50, and the number of iterations is 100. When the number of iterations is less than 75, the probability of each operator being selected is $p(x_1)=0.1$, $p(x_2)=0.1$, $p(x_3)=0.4$, and $p(x_4)=0.4$. When the number of iterations is more than 75, the probability of each operator being selected is $p(x_1)=0.3$, $p(x_2)=0.3$, $p(x_3)=0.2$, and $p(x_4)=0.2$.

2) Scenario 2: Number of work routes more than number of mowing robots

Generally, the more the number of tasks, the more the number of work routes planned by the algorithm. One should consider the situation in which there is a shortage of mowing robots and they cannot complete all the tasks in one trip. So, it is necessary to require a second allocation of work routes. It is assumed that there are three mowing robots in the garage, and the endurance time of each mowing robot is set to 1.2 h. Different methods have been used to assign work routes to the three mowing robots in the hope that they can jointly complete the mowing tasks of 16 plots in the orchard in multiple trips. The tested methods consist of random allocation and the local search algorithm designed in this paper.

Table 5 Coverage time of all nodes

Node number	Coverage time/h	Node number	Coverage time/h
1	1.08	9	0.06
2	0.51	10	0.04
3	0.60	11	0.17
4	0.12	12	0.31
5	0.34	13	0.70
6	0.18	14	0.35
7	0.06	15	0.36
8	0.17	16	0.41

3.3.4 Field experiment validation

To validate the practicability of the proposed algorithms (MC-GA and Mix-ACO) in solving the path planning and task allocation problems, the field experiments were conducted in the Modern Science and Technology Agricultural Park.

Experimental Site: Plot No.5 was selected for the path planning experiments. Its environmental parameters were obtained by taking the average value of several measurements in the field: the number of tracks is 32, the spacing between rows is 3.8 m, the width of the ground cloth is $L_d=2.0$ m, and the angles between the driving direction of the mower and the boundary of the UH and LH headland are $\alpha=83^\circ$, $\beta=90^\circ$. Plots No.1, 2, 3, 4, 5, 6, 7, 10, 14, and 16 were selected for the task allocation experiments. The main purpose of task allocation in this paper is to minimize the total transfer time of mowers when they operate across plots. Therefore, only the transfer time of the mower was to be measured during the experiment, and no additional operations were required. To save resources, this study only used one mower for the experiments.

Experimental indicators: The experimental process is affected by a number of factors, so the operating time (t) and fuel consumption rate (g) of the mower are used as evaluation indicators. The t is timed by a timer, and g is calculated as follows:

$$g = \frac{H_1 - H_2}{H_3} \times 100\% \quad (25)$$

where, H_1 is the height of the fuel tank of the mower before the experiment; H_2 is the height of the fuel tank of the mower after the experiment; H_3 is the height of the fuel tank of the mower when it is full of fuel, which is measured to be 0.32 m.

Experimental process: The experiments were divided into two parts, including the path planning experiments and the task allocation experiments.

The path planning experimental process was as follows: (1) measure and record H_1 ; (2) control the G33 mower to execute adjacent track sequence to cover the entire plot, recording its operational time t ; (3) measure and record H_2 ; (4) repeat steps (1)-(3) to test the operation paths generated by SADG, GA, and MC-GA sequentially.

The task allocation experimental process was as follows: (1) confirm entrances/exits of the selected plots; (2) control the G33 mower to start from the garage to execute the work routes generated by the ACO sequentially, recording its operation time t ; (3) repeat step (2) to test the work routes generated by Mix-ACO.

4 Results and discussion

4.1 MC-GA simulation experiment results

The path experiment results of the reciprocating method and MC-GA are listed in Table 6. The total turning time of the two path planning methods was positively correlated with both the plot area and the robot's turning radius. When the mowing robot used the path planned by the MC-GA, both the total turning time and number of reverses were less compared with executing the reciprocating method. Specifically, the total turning time was reduced by 18.33%-31.85%, while the number of reverses was reduced by 60%-96.43%. This shows that using the MC-GA to optimize the path is very effective. The mowing robot chooses more U-turns after using the MC-GA to optimize the track sequence.

Table 6 Results of path experiments using the reciprocating method and MC-GA

Number	Turning radius r/m	Average total turning time/s		Number of reverses		
		MC-GA	Reciprocating	Reduction rate of total turning time/%	MC-GA	Reciprocating
No.1	0.8	251.74	341.43	26.27	2	28
	0.9	259.07	368.33	29.66	1	28
	1.0	266.91	395.24	32.47	1	28
No.5	0.8	145.85	194.16	24.88	1	16
	0.9	150.80	209.55	28.04	2	16
	1.0	155.77	225.03	30.78	1	16
No.10	0.8	46.11	56.46	18.33	2	5
	0.9	48.65	61.26	20.58	1	5
	1.0	51.20	66.07	22.80	2	5
No.14	0.8	107.21	139.25	23.01	2	10
	0.9	111.55	148.80	25.03	1	10
	1.0	116.01	158.66	26.88	2	10
No.16	0.8	189.53	255.08	25.70	1	2
	0.9	195.44	275.27	29.00	1	21
	1.0	201.35	295.47	31.85	2	21

The total turning time under different turning radius for the same plot was compared, revealing that the optimization effect tends to increase as the turning radius becomes larger. Based on further analysis, this may be because the path planned by the MC-

GA often involves the U-turn, while the path length of the U-turn is less affected by changes in the turning radius. In order to verify this idea, a simulation experiment was conducted on plot No.5, which set the turning radius to range from 0.7 to 1.2 m with intervals of 0.1 m. The turning speed was set to $v_a=v_t=1.1$ m/s to ensure the unicity of variables. The experiment results are listed in Table 7. It can be seen that the results were as expected. When the turning radius gradually increased from 0.7 m to 1.2 m, the average increase in the total turning time of the path planned by the reciprocating method was larger. This indicates that the T-turn is more affected by changes in the turning radius than the U-turn.

Table 7 Results of the total turning time (s) with different turning radius

Turning radius r/m	0.7	0.8	0.9	1.0	1.1	1.2	Average increase of total turning time/s
Method							
MC-GA	136.97	141.12	145.29	149.48	153.71	157.98	4.20
Reciprocating	147.13	156.26	165.47	174.73	184.06	193.53	9.28

The path experiment results of SADG, IPSO, GA, and MC-GA are listed in Table 8. Compared with other algorithms, MC-GA consistently obtained the shortest total turning time in all problems, reducing the total turning time by 11.6%-23.39% and the number of reverses by 66.67%-83.33%. When the problem size was small, such as in the plots No.10 and No.14, both SADG and MC-GA could obtain optimal solutions. However, as the size of the problem increased, this phenomenon gradually disappeared. Meanwhile, IPSO had the worst solution among all the algorithms. The results of 10 simulation experiments for SADG, IPSO, GA, and MC-GA are shown in Figure 9, with standard deviations of 5.423, 5.404, 1.609, and 0.000, respectively. In the process of 10 simulation experiments, MC-GA always obtained the optimal solution, and its results were more stable compared with the other algorithms. The iteration process of each algorithm is demonstrated in Figure 10, and it can be seen that MC-GA has a faster convergence speed and higher optimization efficiency.

Table 8 Results of MC-GA and other algorithms in solving CCPP

Number	Number of tracks	Average total turning time/s		Number of reverses	
		SADG	IPSO	GA	MC-GA
No.1	56	328.63	8	358.74	11
No.5	32	155.00	3	192.77	5
No.10	10	48.65	2	48.65	1
No.14	20	111.55	2	137.63	6
No.16	42	217.86	6	261.5	12
Reduction rate of MC-GA/%		11.16	71.43	23.39	83.33
				19.18	66.67
				-	-

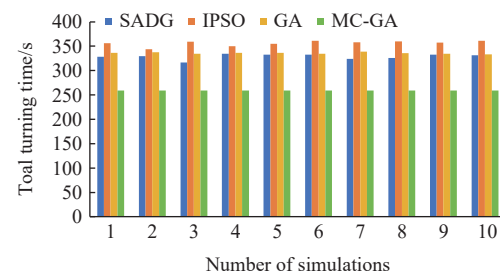


Figure 9 Results of 10 simulation experiments for SADG, IPSO, GA, and MC-GA

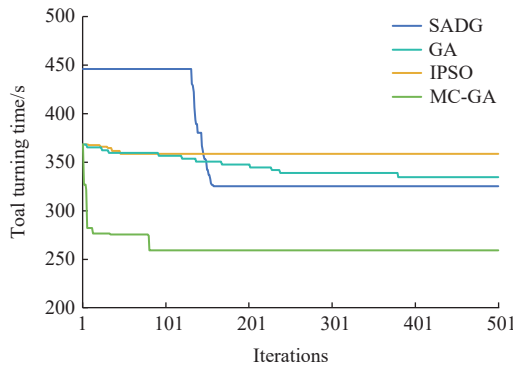


Figure 10 Path optimization efficiency comparison

4.2 Mix-ACO simulation experiment results

The results of the total transfer time between ACO allocation and Mix-ACO allocation under different numbers of tasks and different endurance times of the robot are listed in Table 9. As seen

in Table 9, Mix-ACO can effectively allocate tasks by generating multiple work routes and reduce the non-working time. Mix-ACO planned 2, 2, 4, 5, and 5 work routes, respectively, when the task quantities were set to 4, 7, 10, 13, and 16, and the endurance time of the mowing robot was set to 1.2 h. Compared with ACO allocation, the total transfer time was reduced by 0.00%, 0.32%, 5.72%, 5.38%, and 1.90%, respectively. If the endurance time was set to 1.5 h, Mix-ACO planned 2, 2, 4, 4, and 4 work routes, respectively. The total transfer time was reduced by 0.00%, 0.32%, 3.23%, 2.01%, and 5.37%, respectively. The results of 10 simulation experiments for Mix-ACO and ACO are listed in Figure 11, with standard deviations of 0.011 and 0.010, respectively. From Figure 11, it can be seen that the overall results of Mix-ACO were smaller than those of ACO. The iterative process of Mix-ACO and ACO is shown in Figure 12. It can be seen that ACO was prone to premature convergence, whereas Mix-ACO could search the neighborhood well and find a better solution.

Table 9 Results of ACO allocation and Mix-ACO allocation

Endurance /h	Task quantity	Node number	Number of work routes	Average total transfer time of ACO allocation/h	Average total transfer time of Mix-ACO allocation/h	Reduction rate of total transfer time/%
1.2	4	(1,6,9,14)	2	0.296	0.296	0.00
	7	(2,4,6,8,10,12,15)	2	0.317	0.316	0.32
	10	(1,3,5,7,11,12,13,14,15,16)	4	0.647	0.610	5.72
	13	(1,2,3,4,7,8,9,10,12,13,14,15,16)	5	0.744	0.704	5.38
	16	All nodes	5	0.789	0.774	1.90
1.5	4	(1,6,9,14)	2	0.296	0.296	0.00
	7	(2,4,6,8,10,12,15)	2	0.317	0.316	0.32
	10	(1,3,5,7,11,12,13,14,15,16)	4	0.619	0.599	3.23
	13	(1,2,3,4,7,8,9,10,12,13,14,15,16)	4	0.646	0.633	2.01
	16	All nodes	4	0.707	0.669	5.37

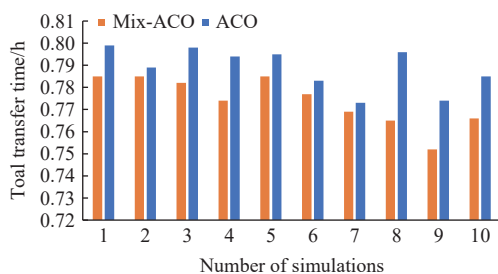


Figure 11 Results of 10 simulation experiments for Mix-ACO and ACO

The experimental results of random allocation and the local search algorithm are listed in Table 10. In the first task allocation, Mix-ACO planned five work routes, which exceeded the actual number of mowing robots. Therefore, the local search algorithm was used for the second task allocation, i.e., five routes were reasonably assigned to three mowers so that the three mowers could complete all tasks in multiple trips. The mowing robot No.1 was responsible for three plots, working with the sequence of plots No.3, 2, and 1, and the task completion time was 2.335 h. The mowing robot No.2 was responsible for ten plots, working with the sequence of plots No.14, 15, 16, 10, 5, 8, 9, 6, 7, and 4, and the task completion time was 2.450 h. The mowing robot No.3 was responsible for three plots, working with the sequence of plots No.11, 12, and 13, and the task completion time was 1.423 h. Node 0 in the work route represents the garage. Therefore, node 0 at both ends of the route respectively means that the robot fleet starts from the garage simultaneously to work and needs to return to the garage

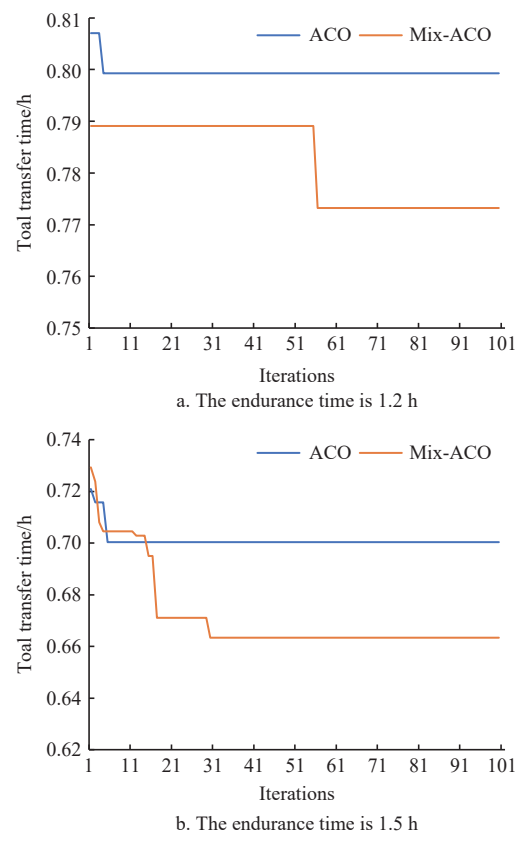


Figure 12 Comparison of optimization process between ACO and Mix-ACO

after completing all tasks. On the other hand, when node 0 appears in the route, it means that the mowing robot must return to the garage to refuel before continuing its work. The work routes of the robot fleet include the work content and work sequence, which realizes the task allocation of collaborative operation of multiple mowing robots. The results of 10 simulation experiments for Mix-ACO&Random and Mix-ACO&LS are shown in Figure 13, with standard deviations of 0.092 and 0.004, respectively. In the process of 10 simulation experiments, the results of the local search

algorithm were better and more stable compared with random allocation. As shown in Figure 14, whether Mix-ACO or ACO was used for the first task allocation, the random allocation results were worse compared with the local search algorithm. Therefore, the mathematical models and algorithms proposed in this paper are effective in reducing the difference in fleet completion time, which is of great help to shorten the overall duration of the robot fleet. This is because the overall duration is determined by the operating time of the mowing robot that is the last one to complete its tasks.

Table 10 Allocation results of the work routes for the three mowing robots

Method	First task allocation		Second task allocation
	Work route1: 0-11-12-13-0	Work route2: 0-14-15-16-10-0	
Mix-ACO&LS	Work route3: 0-5-8-9-6-7-4-0	Work route4: 0-3-2-0	Whole work route for robot 1: 0-3-2-0-1-0
	Work route5: 0-1-0	Work route1: 0-15-14-16-10-0	Whole work route for robot 2: 0-14-15-16-10-0-5-8-9-6-7-4-0
	Work route2: 0-11-12-13-0	Work route3: 0-5-4-7-8-9-6-0	Whole work route for robot 3: 0-11-12-13-0
	Work route4: 0-3-2-0	Work route5: 0-1-0	Whole work route for robot 1: 0-3-2-0-5-4-7-8-9-6-0-1-0
	Work route1: 0-5-4-7-8-9-10-11-6-0	Work route2: 0-13-12-0	Whole work route for robot 2: 0-11-12-13-0
Mix-ACO& Random	Work route3: 0-14-15-16-0	Work route4: 0-3-2-0	Whole work route for robot 3: 0-15-14-16-10-0
	Work route5: 0-1-0	Work route1: 0-5-4-7-8-9-10-11-6-0	Whole work route for robot 1: 0-3-2-0-5-4-7-8-9-10-11-6-0
	Work route2: 0-11-12-13-0	Work route3: 0-5-4-7-8-9-6-0	Whole work route for robot 2: 0-1-0-13-12-0
	Work route4: 0-3-2-0	Work route5: 0-1-0	Whole work route for robot 3: 0-14-15-16-0
	Work route1: 0-5-4-7-8-9-10-11-6-0	Work route2: 0-13-12-0	Whole work route for robot 1: 0-2-5-0
ACO&LS	Work route3: 0-14-15-16-0	Work route4: 0-3-2-0	Whole work route for robot 2: 0-1-0-13-12-11-0-3-8-4-6-7-9-0
	Work route5: 0-1-0	Work route1: 0-5-4-7-8-9-10-11-6-0	Whole work route for robot 3: 0-10-14-15-16-0
	Work route2: 0-11-12-13-0	Work route3: 0-14-15-16-0	
	Work route4: 0-3-2-0	Work route5: 0-1-0	
	Work route1: 0-5-4-7-8-9-10-11-6-0	Work route2: 0-13-12-0	
ACO&Random	Work route3: 0-10-14-15-16-0	Work route4: 0-2-5-0	
	Work route5: 0-1-0	Work route1: 0-5-4-7-8-9-10-11-6-0	
	Work route2: 0-10-14-15-16-0	Work route3: 0-13-12-11-0	
	Work route4: 0-2-5-0	Work route5: 0-1-0	
	Work route1: 0-5-4-7-8-9-10-11-6-0	Work route2: 0-10-14-15-16-0	

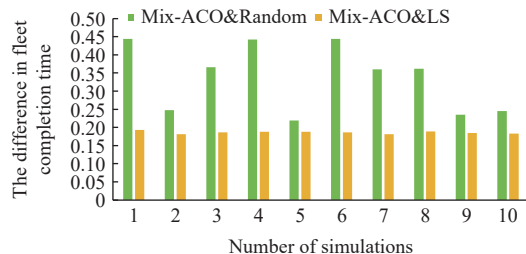


Figure 13 Results of 10 simulation experiments for Mix-ACO&Random and Mix-ACO&LS

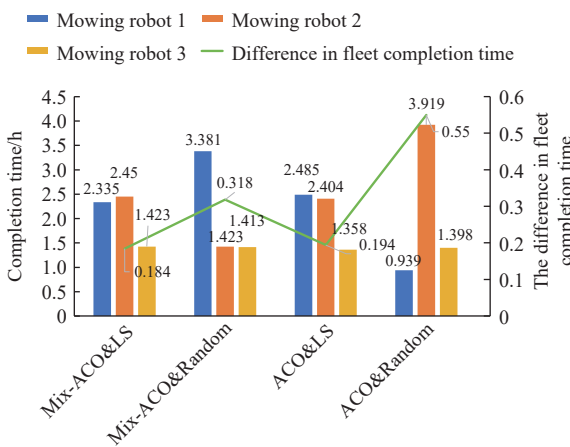


Figure 14 Comparison of task completion time for the three mowing robots

4.3 Field experiment results

The results of the path planning field experiments are listed in Table 11. The G33 mower consumed more fuel and time when using the reciprocating method compared with the algorithms. Among the methods used, MC-GA had the least fuel consumption

and operation time. Compared with the reciprocating method, MC-GA reduced the fuel consumption rate by 8.69% and operation time by 776 s. Compared with GA, MC-GA reduced the fuel consumption rate by 2.64% and operation time by 175 s. Compared with SADG, MC-GA still had an advantage. The results of the task allocation field experiments are listed in Table 12. Mix-ACO can effectively plan work routes based on the plots to be operated, reducing transfer time by 130 s compared with ACO. The field experiment results validate the practicality of MC-GA and Mix-ACO, which can help to reduce the non-working time of the mower.

Table 11 Results of the path planning field experiments

Method	Track sequence	g/%	t/s
Reciprocating	1-2-3-4-5-6-7-8-9-10-11-12-13-14-15-16-17-8-19-20-21-22-23-24-25-26-27-28-29-30-31-32	27.27	3511
SADG	1-3-5-7-9-12-10-13-16-14-17-19-22-24-26-27-30-32-29-31-28-25-23-21-20-18-15-11-8-6-2-4	20.13	2819
GA	1-3-5-2-4-6-8-9-7-10-13-15-12-14-16-17-19-22-20-18-21-24-27-25-28-30-32-29-31-26-23-11	21.22	2910
MC-GA	3-6-8-10-12-14-16-18-20-22-24-26-28-31-29-32-30-27-25-23-21-19-17-15-13-11-9-7-5-2-4-1	18.58	2735

Table 12 Results of the task allocation field experiments

Method	Work routes	t/s
ACO	0-1-5-0	1480
	0-2-3-0	
	0-4-7-6-10-16-14-0	
Mix-ACO	0-1-0	1350
	0-4-3-2-0	
	0-7-10-14-16-6-5-0	

5 Conclusions

This paper proposes a cooperative operation model and method for multiple mowing robots, carrying out path planning and task allocation for the robot fleet. A genetic algorithm with multi-mutation and improved circle algorithm (MC-GA) is proposed to

plan paths. Simulation and field experiments demonstrate the effectiveness of MC-GA. Compared with other path planning methods (reciprocating, SADG, IPSO, GA), MC-GA can effectively reduce the total turning time and fuel consumption of the orchard mower. An ant colony optimization algorithm with mixed operator (Mix-ACO) is proposed for task allocation. Similarly, after experiment verification, compared with ACO, Mix-ACO can allocate tasks reasonably by generating multiple work routes, with a shorter total transfer time of the robot fleet. When the number of work routes exceeds the number of mowing robots, a local search algorithm is proposed to reassign multiple work routes to multiple mowing robots, reducing the difference in fleet completion time. However, this represents only an ideal scenario for multi-machine collaboration, which requires further exploration and improvement. In the next step, unexpected situations arising from the cooperative operation of multiple mowers will be addressed by studying dynamic task allocation methods.

Acknowledgements

This work was funded by the earmarked fund for CARS (CARS-27) and supported by the Earmarked Fund for the Hebei Apple Innovation Team of the Modern Agro-industry Technology Research System (Grant No. HBCT2024150202).

References

- [1] Ren J, Li F D, Yin C B. Orchard grass safeguards sustainable development of fruit industry in China. *J Clean Prod*, 2023; 382: 135291.
- [2] Xie D B, Chen L, Liu L C, Chen L Q, Wang H. Actuators and sensors for application in agricultural robots: A review. *Machines*, 2022; 10(10): 913.
- [3] Ju C, Kim J, Seol J, Son H I. A review on multirobot systems in agriculture. *Comput Electron Agr*, 2022; 202: 107336.
- [4] Mao W J, Liu Z J, Liu H, Yang, F Z, Wang, M R. Research progress on synergistic technologies of agricultural multi-robots. *Applied Sciences*, 2021; 11(4): 1448.
- [5] Zhang W Y, Zeng Y, Wang S F, Wang T, Li H M, Fei K, et al. Research on the local path planning of an orchard mowing robot based on an elliptic repulsion scope boundary constraint potential field method. *Front Plant Sci*, 2023; 14: 1184352.
- [6] Zhang M K, Li X G, Wang L, Jin L J, Wang S B. A path planning system for orchard mower based on improved A* algorithm. *Agronomy*, 2024; 14(2): 391.
- [7] Bochtis D, Griepentrog H W, Vougioukas S, Busato P, Berruto R, Zhou K. Route planning for orchard operations. *Comput Electron Agr*, 2015; 113: 51–60.
- [8] Li T, Xie F, Zhao Z Q, Zhao H, Guo X, Feng Q C. A multi-arm robot system for efficient apple harvesting: Perception, task plan and control. *Comput Electron Agr*, 2023; 211: 107979.
- [9] Albiero D, Garcia A P, Umez C K, de Paulo R L. Swarm robots in mechanized agricultural operations: A review about challenges for research. *Comput Electron Agr*, 2022; 193: 106608.
- [10] Wang N, Yang X, Wang T H, Xiao J X, Zhang M, Wang H, et al. Collaborative path planning and task allocation for multiple agricultural machines. *Comput Electron Agr*, 2023; 213: 108218.
- [11] Zhou J, He Y Q. Research progress on navigation path planning of agricultural machinery. *Transactions of the Chinese Society of Agricultural Machinery*, 2021; 52(9): 1–14. (in Chinese)
- [12] Bochtis D D, Vougioukas S G. Minimising the non-working distance travelled by machines operating in a headland field pattern. *Biosyst Eng*, 2008; 101(1): 1–12.
- [13] Utamima A, Djunaidy A. Agricultural routing planning: A narrative review of literature. *Procedia Computer Science*, 2022; 197: 693–700.
- [14] Filip M, Zoubek T, Bumbalek R, Cerny P, Batista C E, Olsan P, et al. Advanced computational methods for agriculture machinery movement optimization with applications in sugarcane production. *Agriculture*, 2020; 10(10): 434.
- [15] Seyyedhasani H, Dvorak J S. Reducing field work time using fleet routing optimization. *Biosyst Eng*, 2018; 169: 1–10.
- [16] Conesa-Muñoz J, Bengoechea-Guevara J M, Andujar D, Ribeiro A. Route planning for agricultural tasks: A general approach for fleets of autonomous vehicles in site-specific herbicide applications. *Comput Electron Agr*, 2016; 127: 204–220.
- [17] Evans J T, Pitla S K, Luck J D, Kocher M. Row crop grain harvester path optimization in headland patterns. *Comput Electron Agr*, 2020; 171: 105295.
- [18] Ma L, Xin M H, Wang Y J, Zhang Y J. Dynamic scheduling strategy for shared agricultural machinery for on-demand farming services. *Mathematics*, 2022; 10(21): 3933.
- [19] Bochtis D D, Sorensen C G. The vehicle routing problem in field logistics part I. *Biosyst Eng*, 2009; 104(4): 447–457.
- [20] Cao R Y, Li S C, Ji Y H, Xu H Z, Zhang M, Li M Z. Multi-machine cooperation task planning based on ant colony algorithm. *Transactions of the CSAM*, 2019; 50(Supp): 34–39. (in Chinese)
- [21] Wang M, Zhao B, Liu Y C, Wang F Z, Wei L G, Fang X W. Static task allocation for multi-machine cooperation based on multi-variation group genetic algorithm. *Transactions of the Chinese Society of Agricultural Machinery*, 2021; 52(7): 19–28. (in Chinese)
- [22] He P F, Li J, Wang, X. Wheat harvest schedule model for agricultural machinery cooperatives considering fragmental farmlands. *Comput Electron Agr*, 2018; 145: 226–234.
- [23] Utamima A, Reiners T. Navigating route planning for multiple vehicles in multifield agriculture with a fast hybrid algorithm. *Comput Electron Agr*, 2023; 212: 108021.
- [24] Gerkey B P, Matarić M J. A formal analysis and taxonomy of task allocation in multi-robot systems. *The International Journal of Robotics Research*, 2004; 23(9): 939–954.
- [25] Katoch S, Chauhan S S, Kumar V. A review on genetic algorithm: Past, present, and future. *Multimed Tools Appl*, 2021; 80(5): 8091–8126.
- [26] Cao R Y, Li S C, Ji Y H, Zhang Z Q, Xu H Z, Zhang M, et al. Task assignment of multiple agricultural machinery cooperation based on improved ant colony algorithm. *Comput Electron Agr*, 2021; 182: 105993.
- [27] Dorigo M, Stützle T. Ant colony optimization: overview and recent advances. In: Gendreau M, Potvin J-V, editors. *Handbook of Metaheuristics*. Springer. 2019; pp.311–351. doi: [10.1007/978-3-319-91086-4_10](https://doi.org/10.1007/978-3-319-91086-4_10).
- [28] Conesa-Muñoz J, Pajares G, Ribeiro A. Mix-Opt: A new route operator for optimal coverage path planning for a fleet in an agricultural environment. *Expert Systems with Applications*, 2016; 54: 364–378.
- [29] Garcia J, Menchaca R, Sanchez J, Menchaca R. Local search algorithms for the vertex k-center problem. *IEEE Latin America Transactions*, 2018; 16(6): 1765–1771.
- [30] Yao J F, Liu J, Zhang F, Teng G F. Optimization of agricultural machinery operation path based on doppler and greedy strategy. *Journal of Chinese Agricultural Mechanization*, 2020; 41(4): 130–137. (in Chinese)
- [31] Xie J Y, Liu L X, Yang X, Wang X, Wang X S, Chen N. Orchard lawn mower operation path planning based on improved particle swarm optimization algorithm. *Journal of China Agricultural University*, 2023; 28(11): 182–191. (in Chinese)